Assessing Toughness of Pressurized Fluid Channel: Experiment using CTOD in Spiral Submerged Arc Welded Pipes

Hermawan Agus Suhartono
Research Center for Structural Strength Technology, Nasional Research and Inovation Agency, Indonesia

Heryana, Yana
Research Center for Structural Strength Technology, Nasional Research and Inovation Agency, Indonesia

Gilang Cempaka Kusuma
Research Center for Structural Strength Technology, Nasional Research and Inovation Agency, Indonesia

https://doi.org/10.5109/7151771

出版情報：Evergreen. 10 (3), pp.2038-2046, 2023-09. 九州大学グリーンテクノロジー研究教育センター
バージョン：

Assessing Toughness of Pressurized Fluid Channel: Experiment using CTOD in Spiral Submerged Arc Welded Pipes

Hermawan Agus Suhartono[1,*], Yana Heryana[1], Gilang Cempaka Kusuma[1]
[1]Research Center for Structural Strength Technology, Nasional Research and Inovation Agency, Indonesia

*Author to whom correspondence should be addressed:
E-mail: hagussuhartono@yahoo.co.id

(Received May 10, 2023; Revised September 4, 2023; accepted September 7, 2023).

Abstract: This study determines the mechanical properties and Crack Tip-Opening Displacement (CTOD) values for spiral-submerged arc-welding pipes for pressurized fluid channels application. The specimens were tested for mechanical properties, and the CTOD specimens were tested following the ASTM E1820[1)] standard guideline, evaluating weld and base metal. Investigations were conducted on spiral submerged arc welded pipe, revealing good fracture toughness. The base metal exhibits higher CTOD values, indicating superior toughness than the weld metal. The load versus CMOD curve demonstrates a larger plastic region for the base metal than the weld metal. This research confirms the compliance with mechanical properties requirements for API 5L-X70 grade pipeline steels and provides insights into CTOD values for spiral-submerged arc-welding pipe at room temperature.

Keywords: evergreen; crack tip opening displacement, CTOD, spiral welded pipe, toughness

1. Introduction

The use of piping systems in industrial and engineering production is widespread, as they offer a dependable means of transporting diverse fluids and slurries. Acknowledged for their efficiency and effectiveness in liquid transportation, they have become a widely acclaimed method[2)].

The ever-growing demand for increased transportation capacity and stringent safety standards has been instrumental in driving the continuous advancement of pipeline design[3)]. Notably, the manufacturing and progress in high strength low alloy (HSLA) steels have witnessed a remarkable upsurge, mainly driven by this escalating need.

Considerable efforts in research have been conducted to develop high strength low alloy (HSLA) steel. Simion[4)] researched producing electrically welded pipes utilizing micro-alloy steel. On the other hand, Satoshi[5)] introduced a groundbreaking thermo-mechanical control process to make high-performance steel, specifically to meet the ever-increasing demand in the industry.

In the quest for economic competitiveness, developing new alloy options and improving existing ones are essential for the pipeline industry[6)].

Internal pressure in pipeline systems is frequently over 80% of the minimum specified yield strength. Consequently, the susceptibility of pipeline structures to plastic collapse and the propagation of ductile cracks necessitates the incorporation of specific qualities to ensure their integrity. Specifically, in the assembly of thick steel pipes serving as pressurized fluid carriers, the presence of cracks, multi-axial stresses, and stress concentrations due to various loading makes these pipes particularly susceptible to brittle fracture, especially in the vicinity of welded joints. This propensity for brittle fracture might cause fluid leakage and pipeline installation rupture. Under static and fatigue stress circumstances, surface cracks play a critical role in the safety evaluation of the structural pipeline system components[7)]. Strength determines how pipeline steels are categorized. For instance, API X70 steels have nominal yield strengths of 70 ksi or 485 MPa[8)].

Laboratory-scale testing resembling full-scale fracture behavior must be conducted to ensure the structural integrity and safety of construction systems, necessitating a trustworthy fracture control mechanism[9)].

The resistance of a material to crack extension is measured using a fracture toughness test [1]. When plotting variables like K, J, or CTOD versus crack extension, this test may produce a resistance curve or a single value for the fracture toughness[10)].

Security measures involve measuring the strength of the steel material to be used with the CTOD test method to calculate and determine the size of critical defects, enabling the establishment of acceptance standards and

decisions regarding proper non-destructive test evaluation techniques and detection sensitivity before fabrication[11].

The CTOD test is employed as a fracture toughness test when plastic deformation occurs before failure, allowing the stretching and opening of gaps while making quantitative measurements, and it is widely used in engineering applications.

CTOD testing for thick plate classification in welded structures, including pipes, shipbuilding, offshore structures, and pressure vessels, is increasingly popular due to the growing thickness of these structures. Different standards apply acceptable CTOD values to ensure structural safety and stability[12].

Numerous laboratory-scale testing techniques of Crack Tip Opening Displacement (CTOD) testing have been studied to evaluate fracture parameters of steels.

Three distinct types of steels are investigated to compare their mechanical qualities using the CTOD (Crack Tip Opening Displacement) test[13].

Mechanical and welding tests related to preproduction certification are required[14]. Several studies focus on acceptance criteria for CTOD characteristics with variable welding on steel materials, some of which are presented in the following sections.

A study was conducted to analyze the impact of high heat input on the CTOD properties of thick steel plates used in offshore engineering to ensure compliance with CTOD characteristics requirements[15]. The study focused on exploring the CTOD behavior of thick structural E43 steel, which concludes that fracture toughness is significantly influenced by the plastic CTOD of the material[16]. Research by Gordon indicated that biaxial loading in girth welds primarily increases the crack driving force. The material's resistance to fracture under uniaxial and biaxial loading appears to be comparable [17].

Souza's experiment[18] facilitated the development of precise connections between J and CTOD, thus enabling testing procedures for toughness assessments, particularly in analyzing an API X70 steel. On the other hand, Afzalimir's experiment[19] showed that related fracture resistance data based on J-CTOD relationships consistently produced lower findings than CTOD resistance curves based on the double clip-gage (DCG) technique. To calculate pipeline girth welds during reeling installation, particularly during the spooling on and reeling off stages, Permana[20] used software to perform an Engineering Critical Assessment.

Evidence from experiments frequently shows that fractures result from surface imperfections like corrosion, fatigue damage, or welding errors, including undercut, porosity, and slag entrapment[21]. Microbiological activity may have an impact on the corrosion of steel. An investigation was conducted on carbon steel API 5L X65 exposed to microbiologically influenced corrosion (MIC) in a CO2 environment[22].

These flaws propagate through the wall thickness and longitudinally, exhibiting unstable propagation when their length exceeds a critical value[23]. The CTOD methodology is instrumental in determining this critical value, employing notched and pre-cracked samples subjected to static stress to assess material strength in the presence of a crack. These methods enable the determination of critical crack sizes to consider the anticipated increase of crack-like defects during service.

High-strength low alloy (HSLA) steel's toughness is vulnerable to deterioration during pipe manufacturing and installation[11]. The increased ductile-brittle transition temperature results from welding heat cycles and mechanical deformations also cause local brittle zones to form in welded joints at low temperatures and cause brittle failures.

The microstructure significantly influences the mechanical characteristics of welding joints. In addition to granular bainite and acicular ferrite, API X70 steel contains a trace amount of martensite-austenite component (MA). The microstructure of the thermomechanical process contains polygonal ferrite, acicular ferrite, upper bainite (UB), a trace quantity of martensite-austenite component, and cementite[24] under various technological parameters. In addition, quasi-polygonal ferrite, acicular ferrite, granular bainite pearlite, and martensite-austenite component were found in the microstructure of API X70 steel[25]. The bainite phase is harder than ferrite, pearlite, and austenite[26]. Pro eutectoid and Widmanstatten ferrites, as well as acicular ferrite, made up the majority of the microstructure of the Fusion Zone[27].

CTOD testing is commonly conducted on fluid conduit pipes used in areas exposed to low temperatures. The testing on pipes made of carbon steel with varying microstructure variables has been performed to determine the optimal structural form[28]. Notably, pipeline steel welding joints are more prone to fatigue fracture nucleation and propagation due to welding inclusions and flaws acting as stress concentrators, reducing the steel's toughness[29].

The ASTM E1820 standard test method can be used to measure CTOD and determine the fracture toughness of steels. The fracture toughness of an API X70 pipeline steel at room temperature was investigated in this study. Based on the reference temperature characterizing fracture toughness at room temperature. Fractographic tests were performed to evaluate the fracture characteristics of the CTOD specimens.

The CTOD test is vital in determining the need for repairs, enabling more efficient maintenance strategies. By leveraging the insights the CTOD test provides, repairs can be scheduled when necessary, resulting in significant time and cost savings. This approach eliminates unnecessary downtime and avoids premature or unwarranted repairs, thereby reducing overall maintenance expenses associated with maintaining a structure. The findings emphasize the importance of the CTOD test in optimizing maintenance strategies, allowing

for more efficient and cost-effective management of structures while ensuring their long-term integrity.

2. Experimental Procedure

2.1 Materials

Pipe steel of the API 5L-X70 grade with dimensions of 101.6 mm in outer diameter (OD) and 15.49 mm in wall thickness (WT) was the substance under evaluation. One of Indonesia's most used pipe materials for high-pressure oil and gas transportation is API X70 steel. See Fig. 1 for the spiral submerged arc-welding pipe for the API 5L-X70 pipeline.

Tensile bars made from pipe were used to measure the mechanical characteristics of the pipe. Figure 2 (a) depicts the dimensions of the tensile specimens used to test the weld metal, and Figure 2 (b) shows the specimens for the tensile test.

An extensometer is attached to the test object to measure the strain during testing. The mechanical properties of API X70 steel were measured in this study using three longitudinal pipe body tensile specimens—the tensile tests aimed to ascertain the weld metal's tensile strength.

The test samples were cut from a pipe, as shown in Fig. 3a. Fig. 3b depicts the tension test material and the CTOD samples.

All experiments were conducted at ambient temperature. The tensile test was carried out on a 1000 kN Karl Schenk tensile testing machine, and the number of test objects tested was three pieces.

Fig. 1: The pipe before cutting.

The chemical composition of experimental steel in its final form (thermomechanically produced or rolled) (mass percentage,%):

C 0.11, Si 0.18, Mn 1.4, P 0.008, S 0.002, V 0.058, Nb 0.06, Ti 0.009 %, Carbon equivalent (Pcm)% Max 0.2

In comparison to the requirement of API 5 L X70:

C 0.12, Si 0.45, Mn 1.70, P 0.025, S 0.015, (V+ Nb + Ti) shall be ≤ 0.15%, Carbon equivalent (Pcm) % Max 0.25

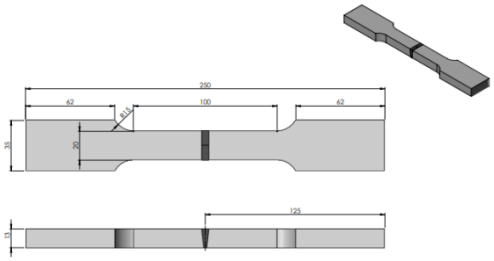

(a)

(b)

Fig. 2: (a) the tensile specimens' dimensions used to test the weld metal; and (b) samples for the tensile test.

2.3 Tests of Toughness CTOD

Specimens for single edge notch bends (SE(B)) were cut from test pipes in the location and manner shown on the schematic in Figure 3.

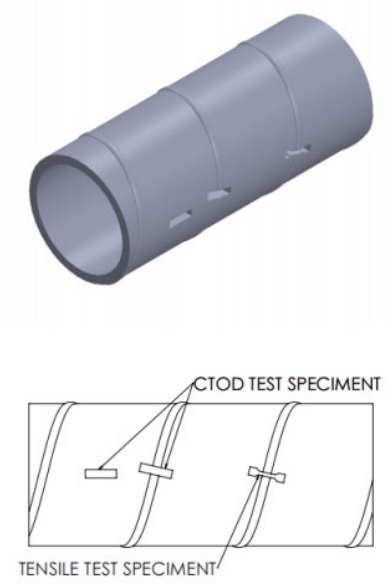

(a)

(b)

Fig. 3: (a) Location and orientation of samples, (b) Material for tension test and CTOD samples.

The ASTM CTOD standards suggest using full section thickness as the specimen size. The specimens were cut, as seen in Fig. 3(a). The samples of the base metal and weld region are shown in Fig. 3(b). Fatigue pre-cracking is required to induce a sharp crack in all specimens 10 and 11. The specimens were pre-cracked using a Schenk Pulser 63 kN with a sinusoidal constant amplitude load, load ratio R = 0.1, at 18 Hz frequency, and at room temperature. To ascertain the initial crack's dimensions following the standard**1)**, as below:

For : $0{,}45 \leq a0 / W \leq 0{,}70$

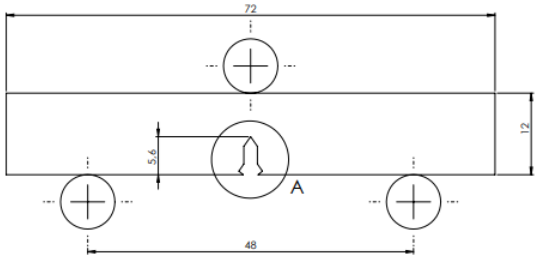

(a)

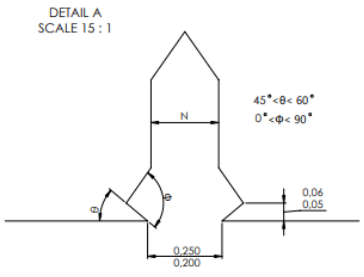

(b)

Fig. 4: (a) Single edge Notched Bending (SENB)1). (b) Dimensions of the notch for initial crack.

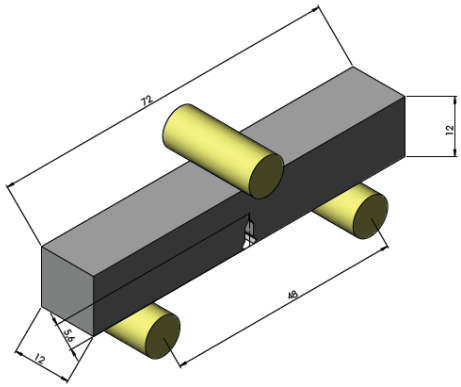

(a)

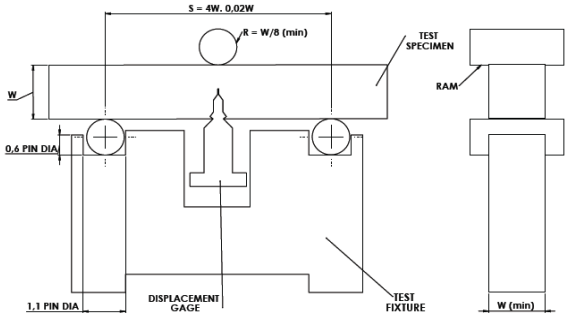

(b)

Fig. 5: (a) Schematic showing the CTOD test and the measurements of the specimen ; (b) Installation of the test specimen on the support of the three-point bending system.

Single edge notch bending (SENB) specimens were used in this test to determine the CTOD in notches located in the weld metal (WM) and base metal, which evaluated the fracture toughness of an API 5L X70 steel.

Figure 4 (a) depicts a specimen for Single Edge Notched Bending (SENB) with the dimensions of the notch for the initial crack shown (b). As indicated in Fig. 4(a), the specimen's dimensions were thickness B =12 mm, width W=12 mm, span S=48 mm, and crack length to width ratio (a/W) of 0.7. It used a knife edge of 2 mm thickness.

Figure 5 shows the dimensions of the test specimen and a schematic for the CTOD test, as well as how the test specimen is installed on a three-point bending system support.

Fatigue pre-cracking is required to create a sharp crack in CTOD specimens. The 63 kN PVQ pulzer testing apparatus is then used to provide a dynamic load (fatigue load) to the CTOD test specimen. The dynamic load is applied this way until the test specimen experiences an initial crack length ≈ of 2 mm. Figures 6a and 6b show the CTOD specimen before and after testing with dynamic load (dynamic crack growth). A fatigue crack is observed initiated from the base of the notch.

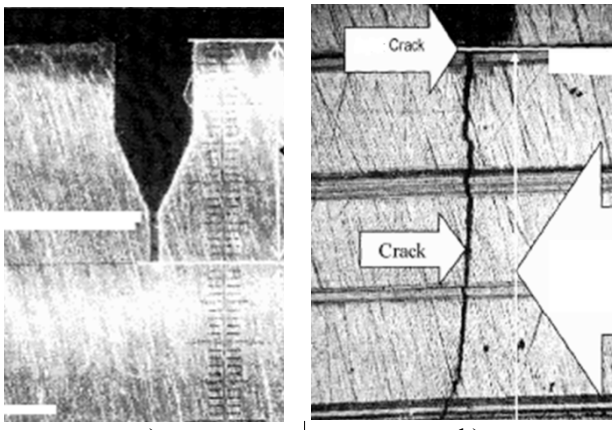

a) b)

Fig. 6: The notch of the CTOD test specimen before dynamic loading and after dynamic loading.

The fracture toughness tests were carried out using the Schenk Universal Testing System RME 100 up to 100 kN with a loading rate that matched the constant crack head displacement of 0.3 mm/min at room temperature. A clip gauge was installed at the top of the knife's notch to measure the displacement of the crack's mouth as a function of the applied stress and to plot the CMOD (Crack Mouth Opening Displacement) versus the applied load. Every sample under examination had a thickness corresponding to the pipe wall thickness as advised by the standards. API-5L. The fracture test was carried out using a room temperature 100 kN RME testing machine. The testing test process for breaking the test object is shown in Fig. 7.

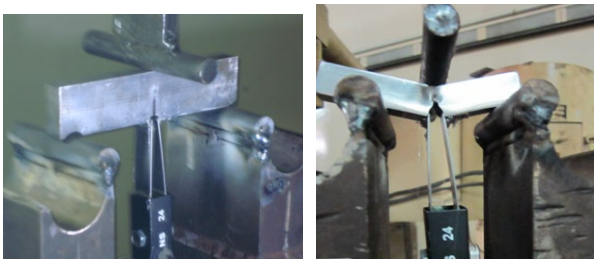

Fig. 7: The process of pressing to break the CTOD specimen

The CTOD value is calculated through the stages of calculating the stress intensity factor, K and Y correction factor[30]. Determination of the stress intensity factor (K) at the end of the fatigue crack on Single Edge Notched Bending (SENB) specimens. , with a three-point bending system testing system, can use the method according to equation (1) as follows:

$$K = YP/\left(BW^{\frac{1}{2}} \right) \quad (1)$$

where:
K = factor of stress intensity
Y = coefficient of stress intensity
P = loading.
B = thickness of the specimen
W = width of specimen

For Single Edge Notched Bending (SENB), the stress intensity coefficient (Y) can be determined by conducting tests with a three-point bending system, where the distance between supports is four times the width of the test object. The calculation of the coefficient of stress intensity (Y) is performed using equations (2) and (3).

For Single edge Notched Bending (SENB), by testing the three point bending system, with a distance between supports of 4 times the width of the test object, the magnitude of the coefficient of stress intensity (Y) is calculated using equations (2) and (3):

$$A = \left(\frac{a_0}{W} \right) \quad (2)$$

a_o= Initial crack length from edge (see fig 1)

$$Y = \frac{6(A)^{\frac{1}{2}} \left(1.99 - A[1-A]\left[2.15 - 3.93A + 2.7A^2 \right] \right)}{(1+2A)(1-A)^{\frac{3}{2}}} \quad (3)$$

The stress intensity coefficient (Y) can be obtained through a table of values derived from comparing the crack length with the width of the specimen using the ratio S/W=41). Once the values of Y are determined, they are then utilized in equations (2) and (3) to calculate the stress intensity factor, K, which is later incorporated into equation (1). Finally, the Crack-Tip Opening Displacement (CTOD) value is computed using equation (4):

$$\delta = \frac{K^2\left(1-\vartheta^2\right)}{2SyE} + \frac{0.4(W-a)V_p}{0.4W+0.6a+z} \quad (4)$$

The above equations are used in calculating the CTOD value in this experiment.Where :

δ is CTOD,
K is the stress intensity factor,
W is the width of the specimen
a is crack length
ϑ is the poison's ratio,
p is the plastic component at critical load,
z represents the clip gage height
Sy is the yield stress under test conditions.
E is Young modulus

The above equations are used in calculating the CTOD

value in this experiment.

3. Result and Discussion

The mechanical properties of API X70 steel, measured from pipeline samples, are shown in Table 1. Each sample showed yield strengths greater than 485 MPa (70 ksi), which met API X70 grade pipeline steel specifications, as seen from the results[8].

Table 1. The tensile characteristics of the specimens at room temperature and the target values.

Pipe Grade	Yield Strength (*YS*) N/mm^2		Tensile Strength (*TS*) N/mm^2		Ratio (Y/T)
X 70 M	Min	Max	Min	Max	
	485	635	570	760	
Spec. 1	506.6		596		0.85
Spec. 2	493.0		574		0.86
Spec. 3	494.7		596		0.83

Following safety protocols, welding connections should have toughness and mechanical properties equal to the base metal. In contrast, weldments with weld metal mechanical strengths greater than the base metal are typically required by modern production standards and procedures (such as ASME and AWS). This criterion aims to reduce the likelihood of structural collapse caused by operational mistakes or unnoticed weld issues. The primary objective of this requirement is to safeguard the integrity of the welded joint against potential negative consequences arising from common weld metal flaws.

During tensile testing, samples cracked in the base metal, demonstrating the superiority of the weld metal's characteristics over the base metal. Due to the base metal typically exhibiting more toughness than the weld metal, the strain may be concentrated there in some instances. Baskoro[31] classified the fracture of welded specimens into two modes: fracture mode 1, which occurs relatively close to the welded area and is influenced by the heat during welding, and fracture mode 2, where the fracture area is relatively far from the welding zone. In this particular tensile testing, the specimen fractured according to fracture mode 2, which is relatively far from the welding area in the base metal. In a study conducted by Baskoro[32], a simulation was developed to visualize heat distribution during welding. This simulation revealed that the highest temperature was concentrated within the molten metal and gradually decreased as it propagated toward the base metal.

For CTOD specimens, fatigue pre-cracking is required to create a sharp crack. The 63 kN PVQ pulzer testing apparatus applies a dynamic (fatigue load) to the CTOD test specimen until it experiences an initial crack length of approximately 2 mm. Figures 6a and 6b depict the CTOD specimen before and after testing with dynamic load, revealing the initiation of a fatigue crack from the base of the notch.

The fracture toughness tests were conducted using the Schenk Universal Testing System RME 100 with a loading rate matching the constant crack head displacement of 0.3 mm/min at room temperature, applying loads up to 100 kN. A clip gage fitted to the top of the knife edge's notch tracked the crack opening as a function of applied stress, creating the CMOD (Crack Mouth Opening Displacement) against the applied load graph. Each sample's thickness followed the pipe wall thickness recommendations of the API-5L standards. Fracture testing was conducted using a 100 kN RME machine at room temperature, as shown in Fig. 7.

Finally, tensile testing was employed for the ultimate breaking to produce the fracture surfaces depicted in Fig. 8, indicating the high toughness qualities of the steel. After completing the CTOD testing, an optical device took crack measurements from the fracture surface. The front fracture in the weld metal sample displayed more irregularities compared to the base metal sample (Figs. 8(a) and 8(b)). Despite this, the samples passed the standard fracture mechanics validation tests.

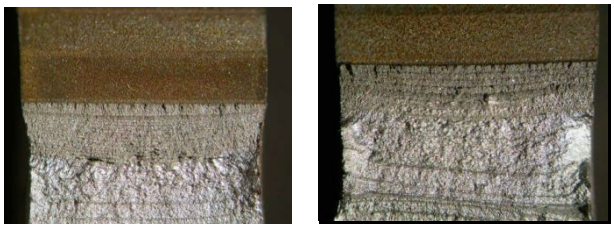

(a) (b)

Fig. 8: Fig. 8: (a) the crack surface of the base metal specimen after the CTOD test. (b) the crack of the surface of the weld metal specimen after the CTOD test.

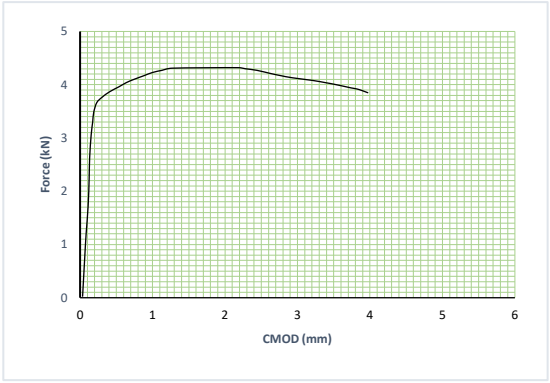

(a)

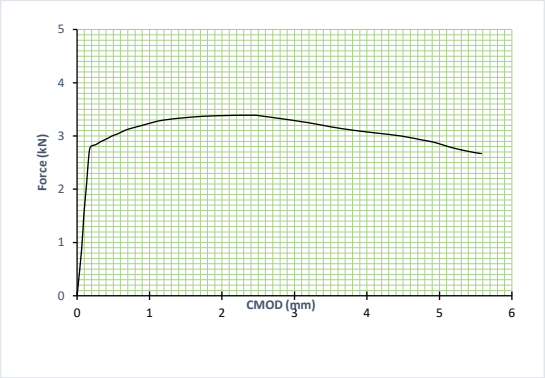

(b)

Fig. 9: (a) Curve Load [kN] versus CMOD [mm] of base metal; (b) Curve Load [kN] versus CMOD [mm] of weld metal.

Figure 9 shows the load [kN] versus displacement or CMOD [mm] curves created for the tested material using the information gathered by the CTOD test apparatus. Figure 9(a) presents the load (kN) versus CMOD (mm) curve for a specimen of the base metal, while Figure 9(b) displays the corresponding curve for a specimen of the weld metal.

The curve in both figures denote the maximum load that the specimen could support (F) as well as the crack mouth opening displacement (CMOD). Also computed was the area integral under the load against the CMOD curve (AP). A maximum load plateau was seen on a load-displacement curve, as shown in Fig. 9, demonstrating that the fracture propagation is still stable after the maximum load, the loading plateau results when the cross-sectional reduction rate and the strain hardening rate are completely balanced.

Table 2. CTOD values determined by ASTM E1820.

Specimens	δ (mm)	$\delta_{average}$ (mm)	St.dev
Weld Metal	0.35	0.32	0.042
	0.29		
Base Metal	0.44	0.40	0.057
	0.36		

The experimental results, comprising the CTOD values for the base and weld metal specimens, are shown in Table 2. According to the findings, the base metal's CTOD value is higher than the weld metal's.

The pipeline steel and its welded joint demonstrated excellent toughness in both samples, exhibiting good toughness at room temperature. Both tested specimens, as depicted in Figs. 8(a) and 8(b) exhibited a high level of flexibility, as evidenced by curves of increasing loads and achieving high values of CMOD. Notably, the CTOD value of the base metal was higher than that of the weld metal, as observed from the load versus CMOD curve. This observation highlighted the base metal's larger plastic region under the curve compared to the weld metal.

Macrostructural observations were conducted in the fracture area, as depicted in Fig. 8, to determine the difference in CTOD values between the test results. The macro photograph revealed that the base metal displayed greater plastic deformation or ductile fracture compared to the weld metal, indicating a higher CTOD value for the base metal.

The microstructures are presented in Figure 10. The base metal's microstructure, which consists of very fine acicular ferrite-bainite grains with an average grain size of the acicular ferrite of 8 μm, is depicted in Figure 10 (a). The welding zone microstructure, which included acicular ferrite and the pro eutectoid ferrite grain boundary phases, is depicted in Figure 10(b). The microstructure, taken from a deeper region within the welding zone, is depicted in Figure 10(c) and comprises grain boundary phases (pro eutectoid and Widmanstatten ferrite) along with acicular ferrite. The acicular ferrite has the highest resistance to fracture propagation brought on by cleavage due to its interlocking structure and small grain size[27].

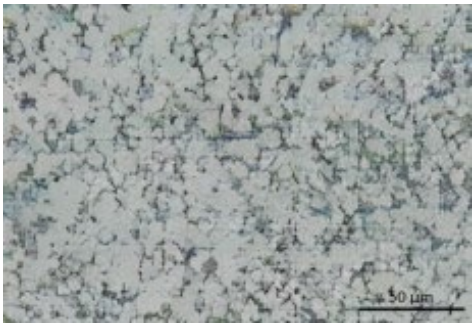

(a)

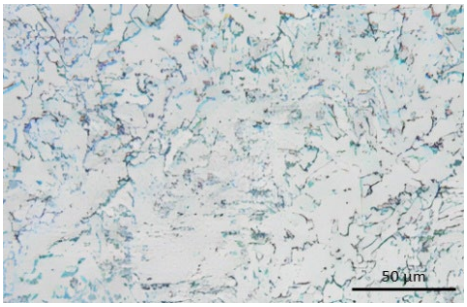

(b)

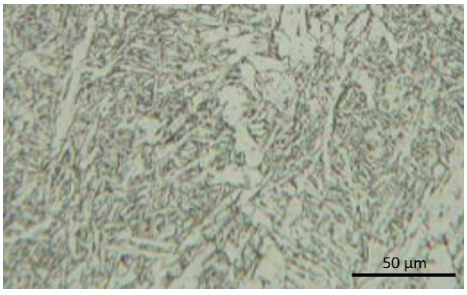

(c)

Fig.10: a) Base metal microstructure, b) Welding Zone microstructure near the surface, c) Welding Zone microstructure in deeper position

CONCLUSION

The conclusions from the investigation are as follows:

1. The tensile test of the weld specimen indicates yield strength and tensile strength meeting API X70 grade requirements of API 5L 44th edition. Specimens broke at base metal during the test, confirming the excellent practice of welding methods.
2. CTOD results show good toughness in both base and weld metal specimens at room temperature. DNV mandates single-value toughness testing in a representative environment with CTODmat ≥ 0.15 mm when fracture toughness reduction uncertainty arises compared to the environment [33].
3. Higher CTOD value in base metal and weld metal underscores its good fracture resistance. These findings enhance comprehension of material behavior in diverse conditions, ensuring safer and more dependable applications in the pipeline sector.
4. The study bears significant industrial implications encompassing material selection, design enhancement, quality control, and failure analysis for such welded pipes

Acknowledgments

The authors are grateful to the National Research and Innovation Agency of the Republic of Indonesia and PT KHI pipe industries for supporting this work.

References

1) ASTM-E1820-20. Standard test method for measurement of fracture toughness. Am Soc Test Mater, p. 1-65, (2020).
2) Yanuar, Ibadurrahman, A. S. Pamitran, Gunawan, Sealtial Mau, "Experimental Investigation On The Spiral Pipe Performance For Particle-Laden Liquids". EVERGREEN Joint Journal of Novel Carbon Resource Sciences & Green Asia Strategy, Vol.7(4) p.580-586 (2020). https://doi.org/10.5109/4150509
3) S. H. Hashemi, "Strength hardness statistical correlation in API X65 steel". *Materials and Science and Engineering A*, Vol. 528(3), p. 1648-1655, (2011).
4) P. Simion, V. Dia, G. Hrițuleac, I. Hrițuleac, C. Munteanu. "Research regarding the Development of Manufacturing of High Frequency Induction Electrical Welded Pipes from Micro-alloy Steel with Good Weldability and Toughness", Advanced Materials Research. (2015).
5) I. Satoshi, M. Masaru, "Development of Thermo-Mechanical Control Process (TMCP) to obtain excellent properties of steel plates, such as high strength, excellent toughness and weldability, JFE TECHNICAL REPORT No. 26, JFE Steel Corporation, (2021).
6) H. Akamine, M. Mitsuhara, M. Nishida, "Developments of Coal-Fired Power Plants: Microscopy Study of Fe-Ni Based Heat-Resistant Alloy for Efficiency Improvement", EVERGREEN Joint Journal of Novel Carbon Resource Sciences & Green Asia Strategy, Vol. 3(2) p.45-53 (2016). https://doi.org/10.5109/1800871
7) R. Brighenti, A. Carpinteri, "Surface cracks in fatigued structural components: a review", *Fatigue & Fracture of Engineering Materials & Structures*, Volume 36, Issue 12, p. 1209-1222, (2013).
8) American Petroleum Institute, Specification for line pipe steel API5L, 44th. ed, Washington D.C, (2008).
9) H. Sung, S. Shin, W. Cha, K. Oh, "Effects of acicular ferrite on charpy impact properties in heat affected zones of oxide containing API X80 linepipe steels," *Materials Science & Engineering A*, Vol. 528(9), p. 3350-3357, (2011).
10) T. L. Anderson, "Fracture mechanics: fundamentals and applications", 2nd ed., CRC: New York, p. 680, (1995).
11) BS 7910:2019 - guide to methods for assessing the acceptability of flaws in metallic structures. BSI Standards Limited, (2019).
12) Total Materia, Critical Crack Tip Opening Displacement (CTOD) Testing: Part Two, (2016), https://www.totalmateria.com/page.aspx?ID=CheckArticle&site=ktn&NM=397
13) Z. Praunseis, P. Virtič, "Evaluation of mechanical properties of soft magnetic materials for axial flux permanent magnet synchronous machines", Przeglą Elektrotechniczny, p.35-37, (2013).
14) American Petroleum Institute. "API recommend practice 2Z", 4th edition, (2005).
15) J. S. Park, B. Jung and J. B. Lee. "Effect of High Heat input on CTOD Property of the Thick Steel Plate for Offshore Engineering." *Posco Technical Report*, (2007).
16) C. Wu, Q.Yu, F. Wang, W. Gong, W. Zhao, "The investigation of fatigue growth and CTOD test of structure steel", IOP Conf. Ser.: Earth Environ. Sci, (2020).
17) J. R. Gordon, G. Keith, and N. C. Gordon, "Defect and strain tolerance of girth welds in high strength pipelines", International Seminar on Welding High Strength Pipeline Steels, CBMM and TMS: USA, p. 365–394. (2013).
18) Y. Sarzosa, D. F. B., Souza, R. F. and C. Ruggieri, "J–CTOD relations in clamped SE (T) fracture specimens including 3-D stationary and growth analysis." *Engineering Fracture Mechanics*, p. 331–354, (2015).
19) S. H. Afzalimir, V. S. Barbosa, C. Ruggieri, "Evaluation of CTOD resistance curves in clamped SE (T) specimens with weld centerline cracks", *Engineering Fracture Mechanics*, Volume 240, (2020).
20) I. Permana, "Study on Engineering Critical Assessment (ECA) of Subsea Pipeline Girth Welds for Reeling Installation" Master Thesis, Faculty of Science and Technology, University of Stavanger, Norway, (2013).
21) M. Paredes, C Ruggieri, "Further results in J and CTOD estimation procedures for SE (T) fracture specimens – Part II: Weld centerline cracks",

Engineering Fracture Mechanics, Oxford, Vol. 89, p. 24 – 39, (2012).
22) R. Zulkafli, N. K. Othman, N. Yaakob, F. K. Sahrani, M. S. H Al-Furjan, "Electrochemical Studies of Microbiologically Influenced Corrosion on API 5L X65 by Sulfate-Reducing Bacteria in CO2 Environments", EVERGREEN Joint Journal of Novel Carbon Resource Sciences & Green Asia Strategy, Vol. 10(1), p.601-607 (2023). https://doi.org/10.5109/6782167
23) H. A. Suhartono , K. Kirman , Y. Prawoto, "On the Influence of the Initial Shear Damage to the Cyclic Deformation and Damage Mechanism", *Metals*, (2022).
24) S. Shin, B. Hwang, S. Lee, N. Kim, S. S. Ahn, Correlation of microstructure and charpy impact properties in API X70 and X80 line-pipe steels. Mater Sci Eng A. (2007).
25) S. S. Sohn, S. Y. Han, J. H. Bae, H. S. Kim, S. Lee, "Efects of microstructure and pipe forming strain on yield strength before and after spiral pipe forming of API X70 and X80 linepipe steel sheets", Mater Sci Eng A. ((2013).
26) W. N. Putra, M. I. A. Widjana, M. Anis, Y. Prasetyo, "The Effect of Transformation Temperature and Holding Time of Bainite Structure Formation on S45C Steel", EVERGREEN Joint Journal of Novel Carbon Resource Sciences & Green Asia Strategy, Vol. 9(4), p.1218-1223, (2022). https://doi.org/10.5109/6625732
27) S. H. Hashemi, D. Mohammadyani, M. Pouranvari, S.M. Mousavizadeh, "On the relation of microstructure and impact toughness characteristics of DSAW steel of grade API X70", Fatigue & Fracture of Engineering Materials & Structures, Blackwell Publishing Ltd. Fatigue Fract Engng Mater Struct, p. 33–40, (2009).
28) M. Kang, H. Kim, S. Lee, S.Y. Shin, "Correlation of Microstructure with Tensile and Crack Tip Opening Displacement Properties at Low Temperatures in API Line pipe Steels". *Met. Mater. Int*., p. 628-638 (2015).
29) M. A. N. Beltrão,, Castrodeza, E. M. and F. L. Bastian, "Fatigue crack propagation in API 5L X-70 pipeline steel longitudinal welded joints under constant and variable amplitudes", *Fatigue & Fracture of Engineering Materials & Structure*, Vol. 34, p. 321-328, (2010).
30) Plaza, L. M, "The Determination of Uncertainties in Critical Crack Tip Opening Displacement (CTOD) Testing", SM & T Standards Measurement & Testing Project No. SMT4-CT97-2165, (2000).
31) A. S. Baskoro, M. A. Amat, R. D. Putra, A. Widyianto, Y. Abrara1, "Investigation of Temperature History, Porosity and Fracture Mode on AA1100 Using the Controlled Intermittent Wire Feeder Method", EVERGREEN Joint Journal of Novel Carbon Resource Sciences & Green Asia Strategy, Vol.7(1) p.86-91 (2020). https://doi.org/10.5109/2740953
32) A. S. Baskoro, M.A. Amat, M.F. Arifardi, "Investigation Effect of ECR's Thickness and Initial Value of Resistance Spot Welding Simulation using 2-Dimensional Thermo-Electric Coupled", EVERGREEN Joint Journal of Novel Carbon Resource Sciences & Green Asia Strategy, Vol. 8(4), p.821-828, (2021). https://doi.org/10.5109/4742127
33) DET NORSKE VERITAS. Submarine Pipelines Systems, Offshore Standards ST-F101, p. 107, (2021).